Regulation of mechanical interactions between fibroblasts and the substratum by stretch-activated Ca^{2+} entry

Steven Munevar[1], Yu-li Wang[1,*] and Micah Dembo[2]

[1]Department of Physiology, University of Massachusetts Medical School, 377 Plantation Street, Suite 327, Worcester, MA 01605, USA
[2]Department of Biomedical Engineering, Boston University, 44 Cummington Street, Boston, MA 02215, USA
*Author for correspondence (e-mail: yuli.wang@umassmed.edu)

Accepted 24 July 2003
Journal of Cell Science 117, 85-92 Published by The Company of Biologists 2004
doi:10.1242/jcs.00795

Summary

Ca^{2+} ions have long been implicated in regulating various aspects of cell movements. We found that stretching forces applied through flexible substrata induced increases in both intracellular Ca^{2+} concentration and traction forces of NIH3T3 fibroblasts. Conversely, application of gadolinium, an inhibitor of stretch-activated ion channels, or removal of extracellular free Ca^{2+} caused inhibition of traction forces. Gadolinium treatment also inhibited cell migration without affecting the spread morphology or protrusive activities. Local application of gadolinium to the trailing region had no detectable effect on the overall traction forces, while local application to the leading edge caused a global inhibition of traction forces and cell migration, suggesting that stretch-activated channels function primarily at the leading edge. Immunofluorescence microscopy indicated that gadolinium caused a pronounced decrease in vinculin and phosphotyrosine concentrations at focal adhesions. Our observations suggest that stretch-activated Ca^{2+} entry in the frontal region regulates the organization of focal adhesions and the output of mechanical forces. This mechanism probably plays an important role in sustaining cell migration and in mediating active and passive responses to mechanical signals.

Movies available on-line

Key words: Cell migration, Focal adhesions, Actin, Vinculin, Lamellipodium

Introduction

Cell migration is important to many crucial biological functions such as embryogenesis, immune responses, wound healing and cancer metastasis (Stossel, 1993). The process involves a number of well-orchestrated steps including protrusion, adhesion, contraction and de-adhesion (Horwitz and Parsons, 1999; Lauffenburger and Horwitz, 1996; Sheetz et al., 1998). Although rapid advances have been made recently in identifying molecular components involved in cell migration, little is known about the mechanism that propels and regulates the movement.

Central to this problem are mechanical interactions between cells and the underlying substratum (Chicurel et al., 1998). Mechanical forces generated by the cell provide the traction for forward migration. For adherent cells such as fibroblasts, strong contractile forces are also required for the detachment of adhesions underneath the cell body and for organizing the extracellular matrix (Cox and Huttenlocher, 1998; Tomasek et al., 2002). In addition to the generation of mechanical forces, an equally important aspect is the ability of cells to sense mechanical signals, such as fluid shear, stretching forces and substratum rigidity (Geiger and Bershadsky, 2001), and to respond by changing their growth rate, morphology and migratory characteristics (Lo et al., 2000; Sai et al., 1999; Tzima et al., 2001; Wang et al., 2000). This interplay between the input and output of mechanical forces probably provides an essential feedback mechanism for guiding cell migration (Munevar et al., 2001b).

Ca^{2+} have long been recognized as an important second messenger for biological processes. In addition to the well-characterized troponin/tropomyosin system of striated muscles, there are multiple Ca^{2+}-sensitive pathways that may play an equally effective role in regulating non-muscle contractility. For example, an earlier study has demonstrated a surge of Ca^{2+} as the eosinophils switch their direction of migration (Brundage et al., 1991). Potential downstream effectors include myosin light chain kinase (Kamm and Stull, 2001), caldesmon (Huber, 1997), gelsolin (Sun et al., 1999) and the Ca^{2+}-activated protease calpain (Glading et al., 2002). However, without a dedicated Ca^{2+} delivery system, such as the T-tubules and sarcoplasmic reticulum in skeletal muscle (Ebashi, 1991), an equally important question is how non-muscle cells regulate Ca^{2+} release for their contractile functions.

Of particular interest with regard to mechano-sensing are the stretch-activated ion channels. Although the molecular identity of these channels is still unclear, electrophysiological studies have clearly demonstrated the entry of extracellular Ca^{2+} upon mechanical stimulation of the plasma membrane (Guharay and Sachs, 1984). A common characteristic of these channels is their dose-dependent sensitivity to the heavy metal blocker gadolinium (Gd) (Yang and Sachs, 1989; Naruse et al., 1998).

The presence of stretch-activated channels has been demonstrated in migrating fish fibroblast-like cells, which respond to stretching forces with a surge in cytoplasmic Ca^{2+} concentration (Lee et al., 1999). A similar Gd^{3+}-sensitive Ca^{2+} surge was observed with human gingival fibroblasts upon mechanical stimulations (Ko et al., 2001). Such stretch-activated channels represent an appealing candidate for mediating mechano-sensitive regulation of mechanical forces, by stimulating contractile forces in response to mechanical forces. Since stretch-activated Ca^{2+} surge appeared to correlate with cell retraction, it was further speculated that stretch-activated channels may function primarily along the cell body, to mediate the retraction and de-adhesion processes (Lee et al., 1999).

We have recently developed traction force microscopy to map mechanical interactions between migrating cells and the underlying substratum (Munevar et al., 2001a). Cells were cultured on flexible substrata impregnated with fluorescent beads, and mechanical forces exerted on the substratum were calculated based on the displacements of beads (Beningo et al., 2001). The flexibility of the substratum also facilitated the application of mechanical forces, by stretching the substratum with a blunt needle, near the cell (Wang et al., 2001). In the present study we have applied this technique to characterize the responses of migrating NIH3T3 fibroblasts to stretching forces. We demonstrate that stretching forces stimulate profound increases in intracellular Ca^{2+} concentration, traction forces and cell migration. Furthermore, Gd^{3+} applied locally to the frontal region of the cell causes a strong inhibition of traction forces and cell migration, while release at the tail has no detectable effect. Our study suggests that a major role of stretch-activated channels is to regulate contractile activities and adhesion structures near the leading edge.

Materials and Methods

Preparation and characterization of polyacrylamide substrata

Thin sheets of polyacrylamide gel were prepared from acrylamide (40% stock w/v; Bio-Rad Laboratories, Hercules, CA) and N,N-methylene-bis-acrylamide (BIS, 2% stock w/v; Bio-Rad) and adhered to activated coverslips as described previously (Beningo et al., 2002; Wang and Pelham, 1998). All the substrata used in this study contained 5% acrylamide, 0.1% BIS and a 1:100 dilution of fluorescent latex beads (0.2 μm FluoSpheres, Molecular Probes, Eugene, OR). The surface was coated covalently with type I collagen using photoactivatable heterobifunctional reagent sulfo-SANPAH (sulfosuccinimidyl 6 (4-azido-2-nitrophenyl-amino) hexanoate (Pierce Chemicals, Rockford, IL), as described previously (Beningo et al., 2002; Wang and Pelham, 1998).

Steady state thickness of the polyacrylamide sheets at 37°C was estimated to be ~75 μm, by focusing a microscope with a calibrated focusing knob from the glass surface to the surface of the polyacrylamide gel. Young's modulus of the polyacrylamide sheets was estimated as 2.8×10^4 N/m^2 as described previously (Lo et al., 2000).

Measurement of traction stress and application of mechanical forces

Traction force microscopy was performed as described recently (Munevar et al., 2001a). Briefly, deformation of the substratum caused by cellular traction forces was determined relative to the relaxed substratum using a pattern recognition algorithm (Margansky et al. 2003). Coordinates defining the deformation field and cell boundary were analyzed with a Bayesian maximum likelihood method, which yielded traction vectors at pre-assigned nodes throughout the cell (Dembo and Wang, 1999). Pseudo-color images were generated by determining the magnitude of the traction stress at each pixel within the cell boundary through interpolation and converting the magnitude into different RGB color combinations. For the application of mechanical stimulation, a blunt microneedle was inserted into the polyacrylamide substratum ~60 μm from a cell, and pulled away from the cell for ~5 minutes (Wang et al., 2001). The force caused displacement of the proximal region of the cell by ~20 μm.

Cell culture and microscopy

NIH3T3 cells were cultured in DMEM (Sigma-Aldrich Chemical, St. Louis, MO), supplemented with 10% donor calf serum (JHR Biosciences, Lenexa, KS), 2 mM L-glutamine, 50 μg/ml streptomycin, and 50 U/ml penicillin (Gibco-BRL, Rockville, Maryland). Polyacrylamide substrata, mounted in open coverslip chambers (McKenna and Wang, 1989), were equilibrated with the culture medium for approximately 30 minutes at 37°C before plating the cells. Phase-contrast images of cells, and fluorescent images of substrata-embedded beads were collected with a 40×/NA 0.75 Plan-Neofluar phase-contrast objective lens on a Zeiss Axiovert S100TV microscope, equipped with a custom stage incubator. Bead images on relaxed substrata were collected at the end of time-lapse recording by removing the cell with a microneedle and micromanipulator (Leitz, Wetzlar, Germany). All images were collected with a cooled CCD camera (ST133 controller with an EEV Type57 back-illuminated frame-transfer CCD chip; Roper Scientific, Trenton, NJ) and processed for background subtraction using custom programs. Time-lapse sequences of cell and bead images were recorded by manually activating slow-scan image acquisition at an interval of 30 seconds to 4 minutes, between which the camera was operated in the video mode to allow precise focusing of the beads and adjustment of the position and flow of the drug release needle (described below).

Fluo-4-dextran (Molecular Probes) was used to monitor intracellular Ca^{2+} concentration. Cells were microinjected with Fluo-4-dextran at 5 mg/ml in 10 mM Tris-acetate (Sigma-Aldrich) and allowed to recover for 30 minutes before the analysis. Interference reflection microscopy (IRM) was performed using a standard epifluorescence illuminator with the emission filter removed.

Pharmacological analysis

Gadolinium was prepared as a 100 mM stock solution from $Gd^{3+}Cl_3$ (Sigma-Aldrich). Manganese was prepared as a 25 mM stock solution from $Mn^{2+}Cl_2$ (Sigma-Aldrich). The stock solutions were diluted in a modified Hank's balanced salt solution (Lee et al., 1999), to obtain working solutions of 100 μM and 500 μM, respectively. Niphedipine (10 μM; Sigma-Aldrich) and EGTA (5 mM; Sigma-Aldrich) were prepared with the same balanced salt buffer. The culture medium was replaced with the drug solution by direct pipetting, and cells were imaged for approximately one hour.

Focal release of Gd^{3+} solution was carried out with a microneedle as described previously (O'Connell et al., 2001). A suction micropipette held 20-40 μm behind the release needle confined the distribution of Gd^{3+} to a region 10-15 μm in diameter. Rhodamine dextran (Molecular Probes) at 5 mg/ml was added to the Gd^{3+} solution to allow monitoring of the distribution of the released solution. The needle was positioned based not on the distance from the cell, but on the distribution of the released solution relative to the cell. The distribution of the solution was checked intermittently during an experiment and the pressure and position adjusted to compensate for pressure fluctuation and tip clogging. Applications of the rhodamine dextran marker alone had no discernable effect on migrating cells.

Immunofluorescence staining

Cells treated with Gd^{3+} or Mn^{2+} for 30 minutes were rinsed with warm PBS with (for phosphotyrosine staining) or without (for vinculin staining) 1 mM sodium orthovanadate (Fisher Scientific, Pittsburgh, PA) and fixed with 4% paraformaldehyde (EM Sciences, Washington, PA) and 0.1% Triton X-100 in warm PBS for 10 minutes. Fixed cells were blocked with 1% bovine serum albumin (BSA; Boehringer Mannheim, Indianapolis, IN) and incubated with vinculin monoclonal antibodies (Vin-11-5, Sigma) or phosphotyrisine monoclonal antibodies (4G10; Upstate Technologies, Lake Placid, NY) at a dilution of 1:100 for 1 hour at 37°C. After thorough washing with 1% BSA in PBS, cells were incubated with Alexa 546-conjugated goat anti-mouse antibodies (Molecular Probes) at a dilution of 1:100 for 45 minutes at 37°C. Counterstaining with fluorescein phalloidin (Molecular Probes) for actin filaments was performed according to the manufacturer's procedure. The intensity of phosphotyrosine staining was quantified by manually defining the boundary of the cell and integrating the fluorescence intensities within the cell boundary. The average intensity outside the cell was subtracted from the average intensity within the cell boundary.

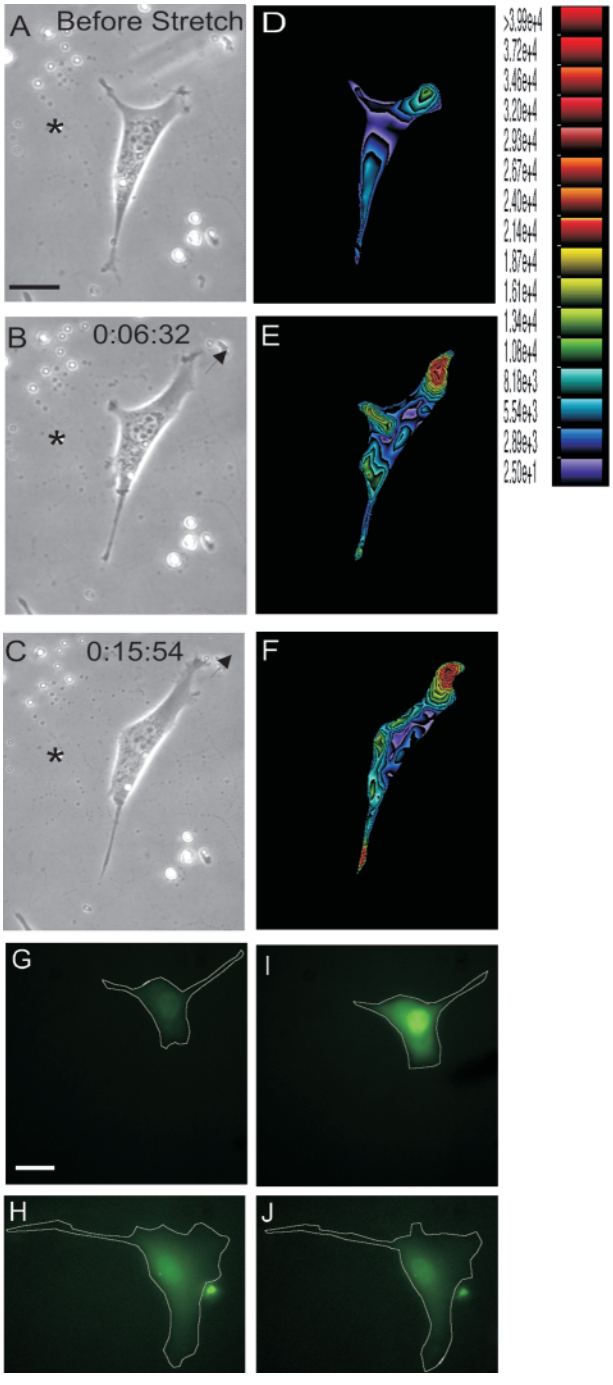

Results

Effects of stretching forces on traction forces and intracellular Ca^{2+}

Previously, we found that stretching forces act as an effective means for guiding NIH3T3 cell migration (Lo et al., 2000). To determine if this process involves an increase in traction forces, we stretched cells on flexible substrata by pulling on the substratum with a microneedle. As shown in Fig. 1, the cell turned toward the direction of stretching forces, accompanied by an increase in traction stress near the leading edge. By comparing the average traction stress magnitude before and after stretching, we found an ~52% increase in traction stress (n=3). We also observed an acceleration of migration from ~0.2 μm/minute to ~0.4 μm/minute, based on the centroid of the nucleus of cells with (n=3) and without stretching (n=6). Furthermore, using cells loaded with the Ca^{2+} indicator Fluo-4, we found that stretching induced an increase in cytoplasmic Ca^{2+} concentration, as indicated by the increase in Fluo-4 intensity (Fig. 1G and I). Owing to the manipulation and the localized defocusing of cells on the flexible substratum during stretching, it was difficult to determine the exact initiation time of Ca^{2+} increase. However, a global increase in intracellular Ca^{2+} concentration was detected as soon as the needle was removed from the substratum. The increase lasted for at least 20 minutes (n=4). These observations suggest that mechanical signals affect the intracellular Ca^{2+} concentration, which may in turn regulate the output of traction forces.

Involvement of stretch-activated channels in Ca^{2+} entry and traction forces

To address whether stretch-activated channels were involved in the mechanical force-induced increase in Ca^{2+}, we treated cells with 100 μM Gd^{3+}, a known blocker of stretch-activated channels (Yang and Sachs, 1989). The treatment inhibited

Fig. 1. Increases in traction forces and intracellular Ca^{2+} following the application of stretching forces. Mechanical forces were applied to a migrating NIH3T3 cell by stretching the flexible substratum near the leading edge with a micro needle. Arrows in B and C indicate the direction of stretching. (A-C) Phase contrast and (D-F) traction stress images were recorded prior to (A,D) and following the removal of the needle, at time points indicated (B,C,E,F). Asterisks mark a fiduciary reference point on the substratum (A-C). Traction stress images were rendered with different colors representing the magnitude, from 2.50×10^1 dynes/cm^2 (violet) to $>3.99\times10^4$ dynes/cm^2 (red). To detect the Ca^{2+} concentration, cells loaded with Fluo-4-dextran were recorded before (G,H) or after (I,J) the application of stretching forces. While the cell stretched in control balanced salt solution showed a clear increase in fluorescence intensity ~10 minutes after stretching (G,I), the cell stretched in 100 μM Gd^{3+} showed a slight decrease in fluorescence intensity (H,J). Scale bars: 20 μm.

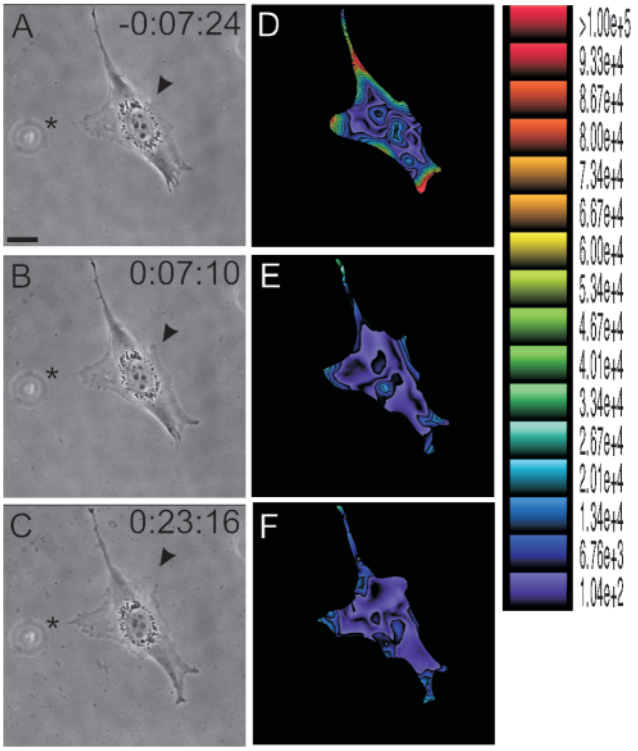

Fig. 2. Response of cell migration and traction forces to the application of Gd^{3+}. Phase contrast images (A-C) of a migrating NIH3T3 fibroblast, recorded before and at specified time points after the application of 100 μM Gd^{3+}. At steady state, the cell showed no apparent effect on the spread morphology or local protrusive activities (arrows, C). However, forward migration of the cell was inhibited. Asterisks mark a fiduciary reference point on the substratum. The corresponding traction stress images (D-F), with different colors representing the magnitude, from 1.04×10^2 dynes/cm^2 (violet) to $>1.00\times10^5$ dynes/cm^2 (red), showed a striking decrease in traction stress following Gd^{3+} application. Scale bar: 20 μm.

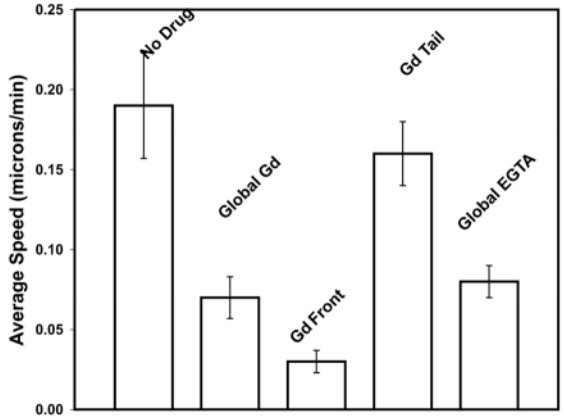

Fig. 3. Average migration speed in response to inhibition of stretch-activated Ca^{2+} entry and Ca^{2+} depletion. NIH3T3 cells incubated globally in gadolinium ion showed a marked decrease in average migration speed compared with control cells. Cell migration speed also decreased sharply upon application of Gd^{3+} to the leading edge, but not when applied to the trailing edge. Global application of EGTA similarly caused a sharp decrease in average migration speed. The rate measured in 5 mM EGTA included some component of nuclear displacement as a result of limited cell retraction. Error bars indicate standard error of the mean.

stretch-activated increase in Ca^{2+} concentration (Fig. 1H and J) (Lee et al., 1999), suggesting that the response must rely on the entry of extracellular Ca^{2+} through stretch-sensitive channels. Treated cells maintained their spread morphology and localized ruffling activities (Fig. 2C), however, the rate of migration decreased as compared with non-treated cells (Fig. 3). Cells incubated in Gd^{+3} also lost their ability to reorient in response to stretching forces (Lo et al., 2000) (n=7). In addition, Gd^{3+} caused traction forces to drop to a basal level within 30 minutes (n=4; Fig. 2D-F), suggesting that Ca^{2+} entry is required for the generation and/or maintenance of traction forces. Cells cultured in balanced salt buffer alone showed no inhibition of traction forces.

Since Gd^{3+} may affect other cellular mechanisms, we have investigated the effects of Ca^{2+} depletion from the medium, which should induce similar effects as those caused by channel blockage. As with Gd^{3+}, chelation of extracellular Ca^{2+} with 5 mM EGTA caused inhibition of traction forces (Fig. 4; n=5), consistent with the notion that entry of extracellular Ca^{2+} is essential for maintaining traction forces. However, EGTA also caused inhibition of ruffling activities and partial retraction, as expected from the involvement of Ca^{2+} in integrin-ECM interactions (Leitinger et al., 2000). Treatment with 10 μM niphedipine, an inhibitor of L-type Ca^{2+} channels that are also believed to be affected by Gd^{+3}, caused no consistent decrease in either traction forces or motility. Together, these results suggest that the entry of extracellular Ca^{2+} is tightly regulated through specific pathways during cell migration, and that stretch-activated channels play a major role in this process.

Previous studies suggested that stretch-activated channels may be involved in regulating the retraction and de-adhesion along the cell body, in response to periodic changes in tension during cell migration (Lee et al., 1999). To determine the site of action of stretch-activated channels, we applied Gd^{3+} locally to different regions of migrating cells with a microneedle while simultaneously monitoring the traction forces. By using fluorescent markers it was determined that the released solution was confined to a region ~15 μm in diameter (O'Connell et al., 2001). We found that only applications to the leading edge caused a decrease in traction forces and cell migration speed (Figs 3 and 5; n=4). Local application of Gd^{3+} to the trailing edge had no detectable effect on traction forces, or cell migration speed during the first 30 min of treatment (Figs 3 and 6; n=4).

Effects of Gd^{3+} on focal adhesions

To assess the mechanism underlying Gd^{3+}-induced inhibition of traction forces, we used IRM to monitor the pattern of adhesion to the substratum. The treatment caused a striking yet transient formation of dark, amorphous contact structures over a large portion of the ventral surface, which may reflect transient interactions of surface negative charges with Gd^{3+} (Fig. 7B, arrows). However, at steady state, treated cells maintained focal adhesion-like structures (Fig. 7C), consistent with their spread morphology despite the strong inhibition of traction forces. Compared to those in control cells, focal

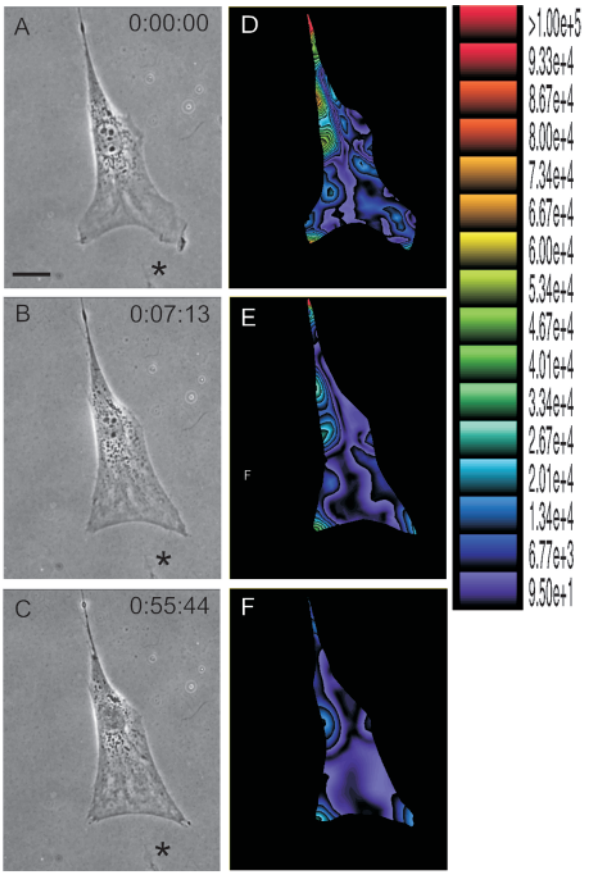

Fig. 4. Response of cell migration and traction forces to the application of EGTA. Phase contrast images (A-C) of a migrating NIH3T3 fibroblast, recorded immediately before (A) and after (B,C) the application of 5 mM EGTA, showed inhibition of local protrusive activities, and partial retraction. Asterisks mark a fiduciary reference point on the substratum. The corresponding traction stress images showed a striking decrease in traction forces (D-F). Different colors represent the magnitude of traction stress, from 9.5×10^1 dynes/cm^2 (violet) to $>1.00\times10^5$ dynes/cm^2 (red). Scale bar: 20 μm.

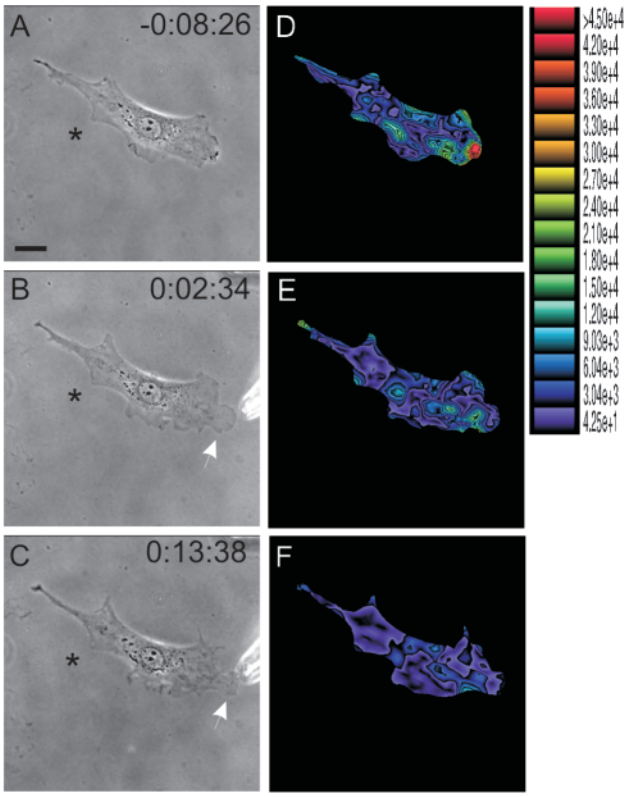

Fig. 5. Response of cell migration and traction forces to local application of Gd^{3+} near the leading edge. Phase contrast images (A-C) of a migrating NIH3T3 fibroblast, recorded immediately before (A) and at specified time points after the application of 100 μM Gd^{3+} near the leading edge (arrows, B,C), showed no inhibition of local protrusive activities (arrows), although the cell body failed to migrate forward. Asterisks mark a fiduciary reference point on the substratum. The corresponding traction stress images (D-F), with different colors representing the magnitude, from 4.25×10^1 dynes/cm^2 (violet) to $>4.50\times10^4$ dynes/cm^2 (red), showed a global decrease in traction stress following the local Gd^{3+} application. Scale bar: 20 μm.

adhesions in Gd^{3+}-treated cells appeared to be less elongated and more centrally localized (compare Fig. 7A with 7C, and Fig. 8I with 8D). There also appeared to be an increase in amorphous close contacts.

To examine the structural organization of focal adhesions in Gd^{3+}-treated cells, we used immunofluorescence to visualize vinculin and phosphotyrosine, and stained actin filaments with fluorescent phalloidin. At focal adhesions, the staining intensity of both vinculin and phosphotyrosine was decreased (Fig. 8A,F,E,J). However, there was some weak vinculin staining at focal adhesions. The total level of phosphotyrosine staining decreased from 1.00×10^3 $\pm2.63\times10^2$ (arbitrary fluorescence unit) before treatment to 6.20×10^2 $\pm2.85\times10^2$ after incubation with Gd^{3+} (n=80). Thus incubation in Gd^{3+} resulted in an approximately 38% decrease in cell tyrosine phosphorylation. Gadolinium-treated cells retained at least some stress fibers, although these fibers were located in the more central region of the cell and were smaller than those in untreated cells (Fig. 8B,G). Treatment of cells with Mn^{2+}, a heavy metal known to increase the integrin-ECM binding affinity, only caused focal adhesions to appear more robust, and no visible difference was found in the IRM morphology of Mn^{2+} treated and control cells (data not shown).

Discussion

Accumulating evidence indicates that cell motility is regulated not only by chemical factors but also by physical parameters. For example, endothelial cells show reorientation along the direction of fluid shear (Shirinsky et al., 1989), while 3T3 fibroblasts migrate preferentially toward stiff substrata or stretching forces (Lo et al., 2000). Such effects probably involve profound changes in the organization of the actin cytoskeleton and/or focal adhesions, as demonstrated by the increase in cortical rigidity (Chicurel et al., 1998; Glogauer et al., 1997), and in vinculin and zyxin concentration at focal adhesions (Riveline et al., 2001; Wang et al., 2001), upon the exertion of mechanical forces on integrin receptors. The mechano-sensitive responses have been implicated in regulating numerous physiological and pathological processes such as embryonic development, wound healing and cancer

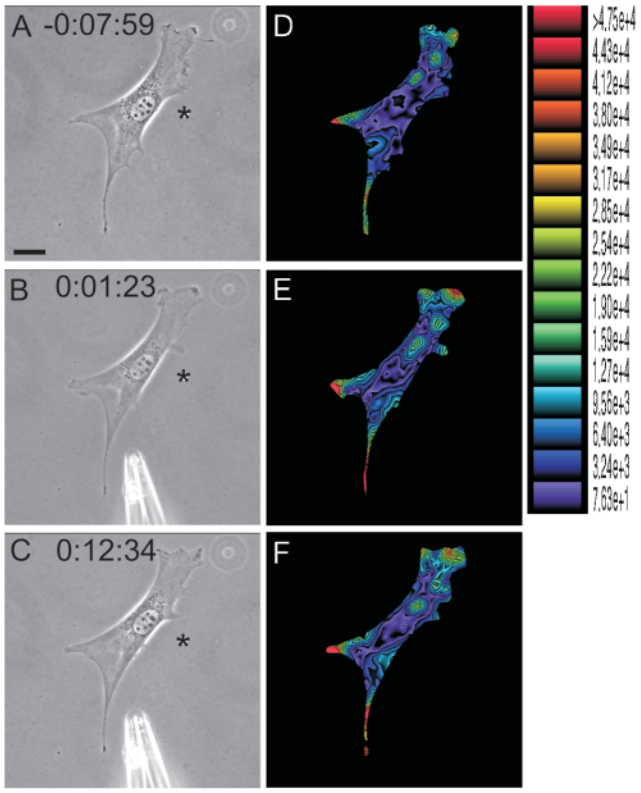

Fig. 6. Response of cell migration and traction forces to local application of Gd^{3+} near the trailing edge. Phase contrast images (A-C) of a migrating NIH3T3 fibroblast, recorded immediately before (A) or at specified time points after the application of 100 μM Gd^{3+} near the trailing edge, showed no apparent effect on cell morphology or migration. Asterisks mark a fiduciary reference point on the substratum. The corresponding traction stress images (D-F), with different colors representing the magnitude, from 7.63×10^{1} dynes/cm^2 (violet) to $>4.75\times10^{4}$ dynes/cm^2 (red), showed no apparent effect on traction stress following the local Gd^{3+} application. Scale bar: 20 μm.

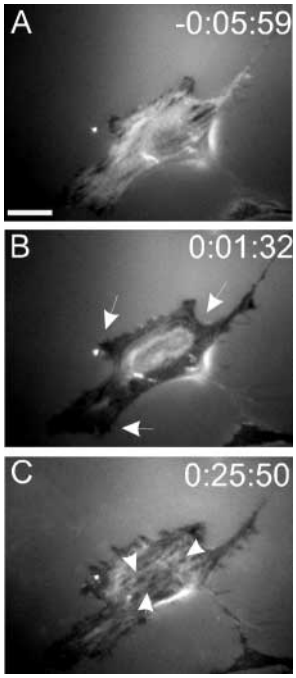

Fig. 7. Response of focal adhesions to Gd^{3+}. IRM images of a NIH3T3 cell were recorded immediately before (A), or after the treatment with 100 μM Gd^{3+} at indicated time points (B,C). Note the transient increase in the darkness of the image (B, arrows), before the image returned to a pattern similar to that before the treatment (C). However, the adhesion plaques appeared less elongated compared with those before treatment, and more adhesion plaques were found near the center of the cell (C, arrows). Also there appeared to be some increase in the amorphous close contact compared to the image before treatment. Scale bar: 20 μm.

metastasis (Ingber, 2002; Rabinovitz and Mercurio, 1996; Tomasek et al., 2002).

The Ca^{2+} ion, with its multiple effects on the actin cytoskeleton, represents an attractive candidate for regulating cell migration. Previous experiments have demonstrated that the reorientation of eosinophils correlates with a surge in cytoplasmic Ca^{2+} (Brundage et al., 1991), while local activation of caged Ca^{2+} induces growth cone turning (Zheng, 2000). In the present study, we showed that Ca^{2+} plays an important role in mechano-sensing and in the generation/transmission of traction forces. We demonstrated that stretching forces caused an increase in intracellular Ca^{2+} concentration, and that such increases were inhibited by the stretch-activated channel blocker Gd^{3+} (Lee et al., 1999). We further demonstrated that the application of stretching forces caused a marked increase, while incubation with Gd^{3+} caused a striking decrease, in cellular traction forces. Furthermore, the results with EGTA, which induced both loss of traction forces and retraction of cells, supported the notion that Ca^{2+} entry through membrane channels is critical for the maintenance of traction forces. The difference between Gd^{3+} and EGTA may be attributed to the disruption of cell adhesion by the removal of extracellular Ca^{2+} (Leitinger et al., 2000), and/or to an inhibition of cell de-adhesion by Gd^{3+} unrelated to its blockage of stretch-activated channels.

Detailed observations further suggested that inhibition of stretch-activated channels alone had no prominent effect on the protrusive activities or the spread morphology. Although the physical contact between cells and the substratum underwent a transient striking increase in close contact, as indicated by the appearance of the dark patches in IRM images (Fig. 7); at steady state there were only subtle differences in IRM images between control and gadolinium treated cells. However, the most intriguing observation was that Gd^{3+} caused a profound reduction of vinculin and phosphotyrosine at focal adhesions. The structural defects may in turn disrupt the mechanical linkage between focal adhesions and the cytoskeleton, leading to the precipitous drop in traction forces and cell migration activities. The decrease in Ca^{2+} may inhibit contractile activities of focal adhesion-associated cytoskeletal structures, causing further dissociation of focal adhesion proteins through inside-out signaling (Burridge and Chrzanowska-Wodnicka, 1996).

Using focal drug delivery (O'Connell et al., 2001), we have investigated the probable sites of action of stretch-activated channels. Previous speculations emphasized the possible regulation of cell de-adhesion and tail release by stretch-activated channels (Lee et al., 1999). It was proposed that cell migration causes tension to rise along the cell body, which in turn opens the stretch-activated channels and triggers tail release. In contrast, we found that local application of Gd^{3+} to the leading edge resulted in a sharp decrease in traction forces and migration rate irrespective of the length of the cell, while applications to the cell body or the trailing edge caused no detectable effect on traction forces. Although Gd^{3+} may have some effects on tail release (Lee et al., 1999), our results suggest that it is the channels at the leading edge that played a dominant role in regulating traction forces and cell migration.

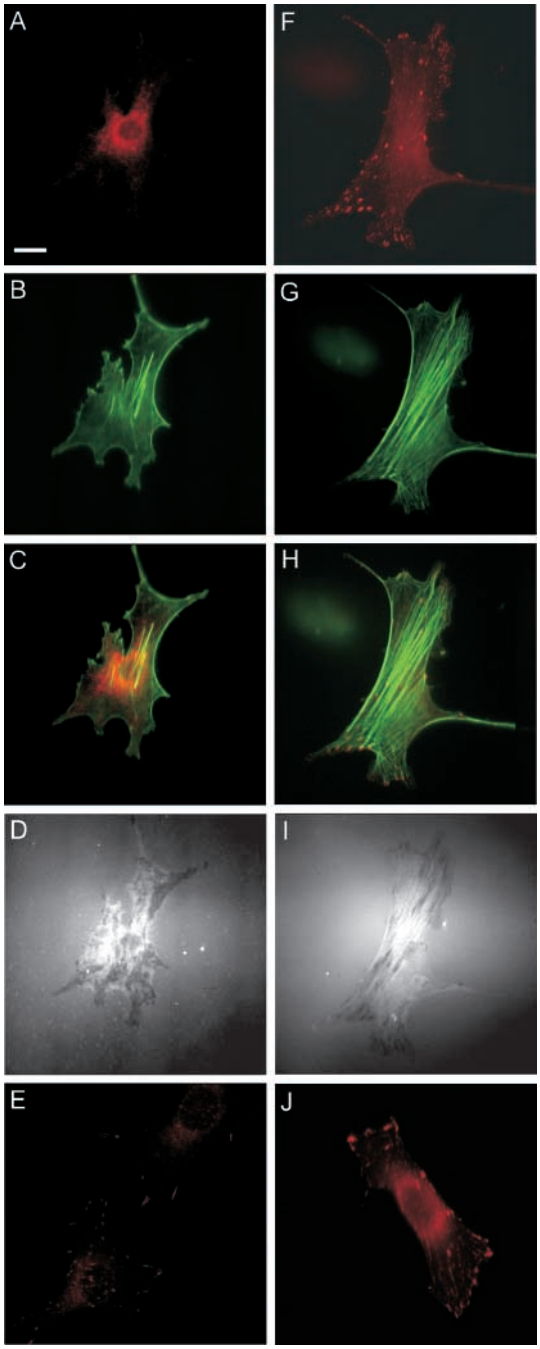

Fig. 8. Effects of Gd^{3+} on vinculin and phosphotyrosine organization. NIH3T3 cells were treated with 100 μM Gd^{3+} (A-E) or control buffer (F-J) for 30 minutes before processing for immunofluorescent staining of vinculin (A,F), actin filaments (B,G), or phosphotyrosine (E,J; in different cells). C and H show combined actin-vinculin images. The control cell showed the characteristic localization of vinculin at focal adhesions (F), which were concentrated at the termini of stress fibers (H) and appeared as dark plaques in the IRM image (I). The Gd^{3+}-treated cell showed a reduction in stress fiber number and intensity, and an increase in cortical actin intensity (B). Short stress fibers persist near the nucleus. Vinculin localization was much reduced at focal adhesions, and appeared primarily perinuclear (A). Staining for phosphotyrosine showed a similar decrease at focal adhesions in Gd^{3+} treated cells (E). IRM image of treated cell showed adhesion plaques throughout the cell (D), which appeared less elongated than those in control cells (I). Scale bar: 20 μm.

Our observations may be understood in the context of the frontal towing model of cell migration (Munevar et al., 2001a). We proposed that the frontal region plays a critical role in both propelling the cell body and responding to guidance cues, whereas the rest of the cell behaves as a passive, resistive cargo. During fibroblast migration, frontal protrusion is followed by the formation of substratum adhesions and the development of active propulsive forces at these nascent focal adhesions (Beningo et al., 2001). The present results suggest that stretch-activated channels have no direct role in the steps of protrusion and substratum adhesion, but profound effects on the development of traction forces and possibly the subsequent maturation of focal adhesions.

In addition, Ca^{2+} entry through stretch-activated channels may be involved in maintaining the migrational directionality, and in mediating both passive and active responses to mechanical signals. Counter forces to the strong traction forces at the front would cause Ca^{2+} entry through stretch-activated channels, which may in turn stimulate the local assembly of focal adhesions and the generation or transmission of traction forces. This mechano-sensitive modulation of mechanical forces would thus provide a positive feedback mechanism to stabilize the polarity of cell migration. Through a similar mechanism, migrating cells would turn toward stretching forces (Lo et al., 2000) (Fig. 1), by stimulating local adhesion structures and traction forces in the stretched region. In addition, resistance of stiff substratum to traction forces may cause a similar opening of stretch-activated channels, and reorientation of the cell (Lo et al., 2000).

A number of intracellular Ca^{2+}-sensitive components may be involved in mediating the stretch response, including the myosin light chain kinase and caldesmon, which are regulated by Ca^{2+}-calmodulin (Walsh, 1994), and gelsolin and non-muscle α-actinin, which are regulated by direct Ca^{2+} binding (Rosenberg et al., 1981; Sun et al., 1999). These proteins are known to affect either the generation of contractile forces or the integrity of the cytoskeletal network for force transmission. However, it is not clear how Ca^{2+} entry affects vinculin and tyrosine phosphorylation at focal adhesions. One attractive mechanism involves the Ca^{2+}-activated protease, calpain (Glading et al., 2002). At least some members of this family of proteases are associated with focal adhesions (Beckerle et al., 1987), and their putative targets include structural and regulatory components such as paxillin and Rho (Geiger and Bershadsky, 2001). Finally, focal adhesions are complex structures containing multiple signal transduction components (Geiger and Bershadsky, 2001). It is probable that the response to stretching forces are modulated by the level of cell-substratum adhesions, and that additional mechano-chemical mechanisms, such as force-induced conformational responses of focal adhesion proteins, function in conjunction with the entry of Ca^{2+} ions. The latter has been suggested in a recent study showing that Triton-extracted cytoskeletons maintained at least some of the abilities to respond to stretching forces (Sawada and Sheetz, 2002).

The authors wish to thank the Boston University Center for Scientific Computing for the use of supercomputer facilities, and Drs Chun-Min Lo, Karen Beningo and Maki Hori for helpful discussions. This project is supported by a NIH research grant GM-32476 to Y.-L.W., and GM-61806 to M.D. S.M. is supported by a NIH NRSA predoctoral fellowship GM-20749.

References

Beckerle, M. C., Burridge, K., DeMartino, G. N. and Croall, D. E. (1987). Colocalization of calcium-dependent protease II and one of its substrates at sites of cell adhesion. *Cell* **51**, 569-577.

Beningo, K. A., Dembo, M., Kaverina, I., Small, J. V. and Wang, Y.-L. (2001). Nascent focal adhesions are responsible for the generation of strong propulsive forces in migrating fibroblasts. *J. Cell Biol.* **153**, 881-888.

Beningo, K. A., Lo, C. M. and Wang, Y.-L. (2002). Flexible polyacrylamide substrata for the analysis of mechanical interactions at cell-substratum adhesions. *Methods Cell Biol.* **69**, 325-339.

Brundage, R. A., Fogarty, K. E., Tuft, R. A. and Fay, F. S. (1991). Calcium gradients underlying polarization and chemotaxis of eosinophils. *Science* **254**, 703-706.

Burridge, K., and Chrzanowska-Wodnicka, M. (1996). Focal adhesions, contractility, and signaling. *Annu. Rev. Cell Dev. Biol.* **12**, 463-518.

Chicurel, M. E., Chen, C. S. and Ingber, D. E. (1998). Cellular control lies in the balance of forces. *Curr. Opin. Cell Biol.* **10**, 232-239.

Cox, E. A. and Huttenlocher, A. (1998). Regulation of integrin-mediated adhesion during cell migration. *Microsc. Res. Tech.* **43**, 412-419.

Dembo, M. and Wang, Y.-L. (1999). Stresses at the cell-to-substrate interface during locomotion of fibroblasts. *Biophys. J.* **76**, 2307-2316.

Ebashi, S. (1991). Excitation-contraction coupling and the mechanism of muscle contraction. *Annu. Rev. Physiol.* **53**, 1-16.

Geiger, B. and Bershadsky, A. (2001). Assembly and mechanosensory function of focal contacts. *Curr. Opin. Cell Biol.* **13**, 584-592.

Glading, A., Lauffenburger, D. A. and Wells, A. (2002). Cutting to the chase: calpain proteases in cell motility. *Trends Cell Biol.* **12**, 46-54.

Glogauer, M., Arora, P., Yao, G., Sokholov, I., Ferrier, J. and McCulloch, C. A. (1997). Calcium ions and tyrosine phosphorylation interact coordinately with actin to regulate cytoprotective responses to stretching. *J. Cell Sci.* **110**, 11-21.

Guharay, F. and Sachs, F. (1984). Stretch-activated single ion channel currents in tissue-cultured embryonic chick skeletal muscle. *J. Physiol.* **352**, 685-701.

Horwitz, A. R. and Parsons, J. T. (1999). Cell migration–movin' on. *Science* **286**, 1102-1103.

Huber, P. A. (1997). Caldesmon. *Int. J. Biochem. Cell Biol.* **29**, 1047-1051.

Ingber, D. (2002). Mechanical signaling. *Ann. New York Acad. Sci.* **961**, 162-163.

Kamm, K. E. and Stull, J. T. (2001). Dedicated myosin light chain kinases with diverse cellular functions. *J. Biol. Chem.* **276**, 4527-4530.

Ko, K. S., Arora, P. D. and McCulloch, C. A. (2001). Cadherins mediate intercellular mechanical signaling in fibroblasts by activation of stretch-sensitive calcium-permeable channels. *J. Biol. Chem.* **276**, 35967-35977.

Lauffenburger, D. A. and Horwitz, A. F. (1996). Cell migration: a physically integrated molecular process. *Cell* **84**, 359-369.

Lee, J., Ishihara, A., Oxford, G., Johnson, B. and Jacobson, K. (1999). Regulation of cell movement is mediated by stretch-activated calcium channels. *Nature* **400**, 382-386.

Leitinger, B., McDowall, A., Stanley, P. and Hogg, N. (2000). The regulation of integrin function by $Ca^{(2+)}$. *Biochim. Biophys. Acta* **1498**, 91-98.

Lo, C.-M., Wang, H.-B., Dembo, M. and Wang, Y.-L. (2000). Cell movement is guided by the rigidity of the substrate. *Biophys. J.* **79**, 144-152.

Marganski, W. A., Dembo, M. and Wang, Y.-L. (2003). Measurements of cell-generated deformations on flexible substrata using correlation-based optical flow. *Methods Enzymol.* **361**, 197-211.

McKenna, N. M. and Wang, Y.-L. (1989). Culturing cells on the microscope stage. *Methods Cell Biol.* **29**, 195-205.

Munevar, S., Wang, Y.-L. and Dembo, M. (2001a). Traction force microscopy of migrating normal and H-ras transformed 3T3 fibroblasts. *Biophys. J.* **80**, 1744-1757.

Munevar, S., Wang, Y.-L. and Dembo, M. (2001b). Distinct roles of frontal and rear cell-substrate adhesions in fibroblast migration. *Mol. Biol. Cell* **12**, 3947-3954.

Naruse, K., Yamada, T. and Sokabe, M. (1998). Involvement of SA channels in orienting response of cultured endothelial cells to cyclic stretch. *Am. J. Physiol.* **274**, H1532-1538.

O'Connell, C. B., Warner, A. K. and Wang, Y.-L. (2001). Distinct roles of the equatorial and polar cortices in the cleavage of adherent cells. *Curr. Biol.* **11**, 702-707.

Rabinovitz, I. and Mercurio, A. M. (1996). The integrin alpha 6 beta 4 and the biology of carcinoma. *Biochem. Cell Biol.* **74**, 811-821.

Riveline, D., Zamir, E., Balaban, N. Q., Schwarz, U. S., Ishizaki, T., Narumiya, S., Kam, Z., Geiger, B. and Bershadsky, A. D. (2001). Focal contacts as mechanosensors: externally applied local mechanical force induces growth of focal contacts by an mDia1-dependent and ROCK-independent mechanism. *J. Cell Biol.* **153**, 1175-1186.

Rosenberg, S., Stracher, A. and Burridge, K. (1981). Isolation and characterization of a calcium-sensitive alpha-actinin-like protein from human platelet cytoskeletons. *J. Biol. Chem.* **256**, 12986-12991.

Sai, X., Naruse, K. and Sokabe, M. (1999). Activation of pp60(src) is critical for stretch-induced orienting response in fibroblasts. *J. Cell. Sci.* **112**, 1365-1373.

Sawada, Y. and Sheetz, M. P. (2002). Force transduction by Triton cytoskeletons. *J. Cell Biol.* **156**, 609-615.

Sheetz, M. P., Felsenfeld, D. P. and Galbraith, C. G. (1998). Cell migration: regulation of force on extracellular-matrix-integrin complexes. *Trends Cell Biol.* **8**, 51-54.

Shirinsky, V. P., Antonov, A. S., Birukov, K. G., Sobolevsky, A. V., Romanov, Y. A., Kabaeva, N. V., Antonova, G. N. and Smirnov, V. N. (1989). Mechano-chemical control of human endothelium orientation and size. *J. Cell Biol.* **109**, 331-339.

Stossel, T. P. (1993). On the crawling of animal cells. *Science* **260**, 1086-1094.

Sun, H. Q., Yamamoto, M., Mejillano, M. and Yin, H. L. (1999). Gelsolin, a multifunctional actin regulatory protein. *J. Biol. Chem.* **274**, 33179-33182.

Tomasek, J. J., Gabbiani, G., Hinz, B., Chaponnier, C. and Brown, R. A. (2002). Myofibroblasts and mechano-regulation of connective tissue remodeling. *Nature Rev. Mol. Cell. Biol.* **3**, 349-363.

Tzima, E., del Pozo, M. A., Shattil, S. J., Chien, S. and Schwartz, M. A. (2001). Activation of integrins in endothelial cells by fluid shear stress mediates Rho-dependent cytoskeletal alignment. *EMBO J.* **20**, 4639-4647.

Walsh, M. P. (1994). Calmodulin and the regulation of smooth muscle contraction. *Mol. Cell Biochem.* **135**, 21-41.

Wang, H.-B., Dembo, M. and Wang, Y.-L. (2000). Substrate flexibility regulates growth and apoptosis of normal but not transformed cells. *Am. J. Physiol.* **279**, C1345-1350.

Wang, H.-B., Dembo, M., Hanks, S. K. and Wang, Y.-L. (2001). Focal adhesion kinase is involved in mechanosensing during fibroblast migration. *Proc. Natl. Acad. Sci. USA* **98**, 11295-11300.

Wang, Y.-L. and Pelham, R. J., Jr (1998). Preparation of a flexible, porous polyacrylamide substrate for mechanical studies of cultured cells. *Methods Enzymol.* **298**, 489-496.

Yang, X. C. and Sachs, F. (1989). Block of stretch-activated ion channels in Xenopus oocytes by gadolinium and calcium ions. *Science* **243**, 1068-1071.

Zheng, J. Q. (2000). Turning of nerve growth cones induced by localized increases in intracellular calcium ions. *Nature* **403**, 89-93.